Theoretical studies of CO hydrogenation to methanol over Cu, Pd, and Pt metals

Chak-Tong Au [a,*], Tai-Jin Zhou [a,b] and Wu-Jiang Lai [a,b]

[a] *Department of Chemistry, Hong Kong Baptist University, Kowloon, Hong Kong, PR China*
E-mail: pctau@hkbu.edu.hk
[b] *Department of Chemistry, Xiamen University, Xiamen 361005, PR China*

Received 11 March 1999; accepted 26 August 1999

Theoretical studies of CO hydrogenation to methanol over Cu, Pd, and Pt metals have been carried out using a quasi-relativistic density-functional method. The metal surface is simulated by a M_{10} cluster model. Reaction energies for the elementary steps involved are determined. The activation energies are estimated by the analytic BOC-MP formula. The results support that these metals are active in CO hydrogenation to methanol. The rate-determining steps are shown to be different for the metals. The highest activation energies of reaction on the metals fall in the order Cu $<$ Pd $<$ Pt, which corresponds to the order of the catalytic activities of the metals in CO hydrogenation.

Keywords: CO hydrogenation, methanol synthesis, quasi-relativistic density-functional method, Amsterdam density-functional program, Cu, Pd, and Pt metal clusters

1. Introduction

The hydrogenation of CO to methanol is an important catalytic process:

$$CO + 2H_2 \rightarrow CH_3OH \tag{1}$$

Two major catalyst systems, viz. supported Cu and Pd catalysts, exhibit high activity and selectivity [1,2]. Methanol can also be produced when supported Pt, Ir, and Rh are used [3,4]. Ternary compositions $Cu/ZnO/Al_2O_3$ and $Cu/ZnO/Cr_2O_3$ are important catalysts used in the industry of methanol synthesis. Because the process is of great commercial importance, considerable efforts have been devoted to the elucidation of the mechanistic details. However, controversies exist in the literature about the reaction mechanism and the chemical state of the Cu component (whether ionic or metallic copper is the catalytically active species). Concerning the mechanism, two general reaction schemes have been proposed [5]. One is the dissociative mechanism in which all CO molecules are assumed to dissociate to surface C and O atoms which then recombine with H to produce methanol. This mechanism was originally proposed by Fischer and Tropsch [6] and has received strong support from several directions based on experimental evidence [7–10]. The other is the non-dissociative mechanism in which adsorbed CO does not undergo dissociation but instead undergoes stepwise hydrogenation. Evidence for this was provided by Koduzono et al. [11]. Especially, the isotopic study of Takeuchi and Katzer [12], who used Rh/TiO_2 in a laboratory study, provided convincing proof that CO remains undissociated during the course of catalysed conversion. The non-dissociative mechanism is also supported by theoretical investigations based on the semi-empirical BOC-MP approach [13]. The BOC-MP calculations indicate that the mechanism of CO hydrogenation depends on the metal used. On metals such as Pd, Pt, and Rh, the activation energies for CO dissociation are very high and C–O bond cleavage on these metals is unlikely to occur. In contrast, other metals such as Ni, Fe, and Ru favor CO dissociation. The hydrogenation of CO on the latter metals produces only hydrocarbons and not methanol.

There is also controversy concerning the active catalytic species [14]. Herman et al. [15] suggested a Cu^+ solution in ZnO as active phase where Cu^+ non-dissociatively chemisorbs and activates CO and ZnO activates H_2. However, Andrew [14,16] presented a case for Cu^0 being the only active component and the role of ZnO was to adsorb poisons present in the syngas. Chinchen et al. [17] found linear dependence of synthesis activity on the surface area of the metallic copper, strongly suggesting that metallic copper is the active phase of the catalyst. This is supported by *in situ* X-ray photoelectron spectroscopy [1] and surface X-ray diffraction studies [18]. Studies of Raney Cu–Zn catalysts [19] have also shown that the active component is the metallic Cu.

In this paper, we attempt to carry out theoretical studies of CO hydrogenation to methanol on three metals (M): Cu, Pd, and Pt. On the basis of the assumption that M^0 is the main active site, all effects of supporting materials on the reaction are neglected in the calculations. We believe that on these metals, methanol is formed via a non-dissociative mechanism.

---

[*] To whom correspondence should be addressed.

© J.C. Baltzer AG, Science Publishers

The paper is organized as follows. Computational method and models are given in section 2. The adsorption properties of intermediate fragments (CO, H, COH$_j$, where $j = 0$–3) and the energetics for the reaction steps involved are discussed in section 3. Our conclusions are summarized in section 4.

2. Computation method and surface modeling

The quantum-chemical calculations were carried out using the Amsterdam density-functional (ADF) program package developed by Baerends and co-workers [20]. The frozen-core approximation was used here to reduce the computational cost. For C and O, the 1s shell was frozen. For the metal atoms, the electrons up to and including $(n-1)$p shells were kept frozen. The valence shells, i.e., $(n-1)$d–ns for the metal atoms, 2s–2p for C and O, 1s for H are expanded in triple-zeta STO basis sets extended by single-zeta STO sets for the inner core wiggles and by single-zeta polarization function (np for the metals, 3d for C and O, 2p for H). The exchange–correlation potential used was based on the density-parametrized form of Vosko, Wilk and Nusair (VWN) [21]. The non-local corrections used were based on Becke's gradient functional for exchange [22] and Perdew's gradient functional for correlation [23]. These corrections are included in a self-consistent manner. Relativistic corrections of the valence electrons were calculated using the quasi-relativistic method due to Ziegler et al. [24].

We chose metal M(111) as the surface for adsorption. M(111) is simulated by a two-layer-thick $M_{10}(n_1, 10-n_1)$ cluster which contains n_1 metal atoms in the first layer and $10-n_1$ in the second. Here n_1 is 7 or 3, depending on the model (on-top size model or three-fold hollow site model) used. It has been shown [25] that a M_{10} cluster is suitably large to give reliable results.

The geometries for the intermediate fragments adsorbed on the metal surface are shown in figure 1. The molecular parts above the surface were fully optimized under certain symmetries (C_{3v} for adsorbed H_2, H and CO; C_s for adsorbed COH$_j$). The M_{10} cluster geometries were held fixed in the calculations, and the M–M distances were based on bulk crystal data.

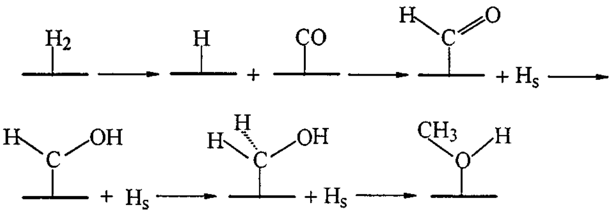

Figure 1. Geometries for the intermediate species adsorbed on the metal surface.

3. Results and discussion

According to the non-dissociative mechanism, the synthesis reaction proceeds by successive hydrogenation of CO to form the corresponding intermediates (see figure 1; s = surface):

$$H_{2,g} \rightarrow 2H_s \tag{2}$$

$$CO_g \rightarrow CO_s \tag{3}$$

$$COH_{j,s} + H_s \rightarrow COH_{j+1,s} \quad (j = 0\text{–}3) \tag{4}$$

The aim of the present study is to examine the energetics of the CO hydrogenation steps. First we begin with the adsorption energies of the various species in reactions (2)–(4). The data are shown in table 1. Table 2 gives the calculated heights of the species above the metal surfaces. Table 3 gives the Mulliken charge distributions on the whole adsorbed species.

3.1. Adsorption energies of intermediate fragments

3.1.1. Adsorbed H

H favors the hollow site on the metals, in agreement with the BOC-MP prediction that a high-coordination site is always preferred for atoms [26]. However, the calculations show that for M = Pd and Pt, there is only small difference (0.1–0.2 eV) in the adsorption energies (E_{ad}) between the on-top and hollow sites. Experimental E_{ad} values of H on M(111) at low coverage are available for the three metals; they are 56 kcal/mol (2.43 eV) [27], 62 kcal/mol (2.69 eV) [27], and 61 kcal/mol (2.65 eV) [28], for M = Cu, Pd, and Pt, respectively. The calculated values are all close to the experimental ones, the errors being less than 0.3 eV.

Table 1
Calculated adsorption energies[a] E (eV) for various species adsorbed on the $M_{10}(n, 10-n)$ cluster model of M(111).

	Cu(7,3) (top)	Cu(3,7) (hol)	Exptl	Pd(7,3) (hol)	Pd(3,7) (top)	Exptl	Pt(7,3) (top)	Pt(3,7) (hol)	Exptl
H	1.32	2.12	2.43	2.27	2.44	2.69	2.58	2.67	2.65
CO	0.55	0.01	0.63	0.90	1.43	1.47	1.17	1.74	1.48
HCO	1.10	1.11		2.45	2.13	(1.91)[b]	2.63	2.18	(1.73)
HCOH	0.84	1.28		2.13	2.31		2.69	3.08	
H_2COH	1.07	1.02		2.16	1.35	(1.86)	2.52	1.65	(1.73)
H_2COH	0.38	0.00		0.46	0.00	(0.48)	0.51	0.00	(0.48)

[a] Experimental data on M(111) are those cited in [27–31].

[b] The value in parentheses is the BOC-MP result [26]; the same is true for the other values in parentheses.

Table 2
Calculated heights (Å) above the metal surface.

	Cu(7,3) (top)	Cu(3,7) (hol)	Pd(7,3) (hol)	Pd(3,7) (top)	Pt(7,3) (top)	Pt(3,7) (hol)
H	1.54	0.94	1.53	0.78	1.57	0.95
CO	1.99	2.63	1.88	1.40	1.90	1.41
HCO	2.03	1.52	1.95	1.48	2.01	1.52
HCOH	1.96	1.41	1.88	1.36	1.92	1.34
H_2COH	2.11	1.74	2.08	1.85	2.14	1.79
H_3COH	2.20	–	2.20	–	2.25	–

Table 3
Mulliken charge distributions (in e) on the whole adsorbed species.

	Cu(7,3) (top)	Cu(3,7) (hol)	Pd(7,3) (hol)	Pd(3,7) (top)	Pt(7,3) (top)	Pt(3,7) (hol)
H	−0.14	−0.07	−0.40	−0.14	−0.55	−0.66
CO	0.20	−0.02	−0.16	−0.53	−0.48	−0.80
HCO	0.06	−0.50	−0.19	−0.67	−0.42	−1.00
HCOH	0.22	−0.42	−0.21	−0.90	−0.49	−1.54
H_2COH	−0.07	0.01	−0.17	−0.44	−0.45	−0.74
H_3COH	0.14	–	0.08	–	−0.22	–

3.1.2. Adsorbed CO

For the adsorption of CO, the bonding sites are not the same for the metals. On Cu, the on-top site is preferred, while the hollow site is preferred on Pd and Pt. The differences in E_{ad} between on-top and hollow sites are ca. 0.55 eV. Experimental adsorption energies are also known for these metals. Again, the calculated and experimental data are in good agreement with the experimental data at low coverage [29–31]. It is shown that the adsorption energy of CO on Cu is significantly smaller than those on Pd and Pt. This is in contrast to the H case. In fact the binding of CO to Cu is rather weak.

3.1.3. Adsorbed COH_j

For the adsorptions of COH_j, there are in fact two coordination modes, viz. the coordination of COH_j via C or O. We find that for HCO, HCOH, and H_2COH, the coordination via C is more favorable; for H_3COH, the preferred coordination is that via O (see figure 1). The calculated adsorption energies of HCO and H_2COH on Cu on-top and hollow sites are nearly equal. The difference in energy may be too small for one to make a definite assignment of the bonding site on Cu. On Pd and Pt, the two species favor the on-top site. For the adsorption of HCOH, the hollow site is preferred universally, contrary to the HCO and H_2COH cases. We note that HCO and H_2COH are monovalent radicals, whereas HCOH is a divalent one. Therefore, unsaturated C in these species has a tendency to recover its missing bonds, in agreement with the extended Hückel band prediction [27]. The three species can be rather strongly adsorbed on the metals. The calculated adsorption energies are 1–1.3 eV on Cu, 2.3–2.5 eV on Pd, and 2.6–3.1 eV on Pt.

Because H_3COH is a saturated molecule, the adsorption energy of this species is small. The on-top site is more preferred than the hollow site for the adsorption, which supports the point of view [26] that for a saturated molecule, one can assume the on-top coordination.

3.2. The CO hydrogenation reactions

The calculated adsorption energies given in table 4 together with the calculated H–C or H–O binding energy in the gas-phase COH_{j+1} can be used to determine the combination energy for reaction (4). The scheme is shown as follows:

$$\begin{tikzcd} \mathrm{COH}_{j,\mathrm{s}} & +\,\mathrm{H_s} \arrow[r, "C_{\mathrm{A+B,s}}"] & \mathrm{COH}_{j+1,\mathrm{s}} \\ \mathrm{COH}_{j,\mathrm{g}} \arrow[u, "-E_{\mathrm{A}}"'] & +\,\mathrm{H_g} \arrow[u, "-E_{\mathrm{B}}"'] \arrow[r, "C_{\mathrm{A+B,g}}"'] & \mathrm{COH}_{j+1,\mathrm{g}} \arrow[u, "-E_{\mathrm{AB}}"'] \end{tikzcd} \qquad (5)$$

$$C_{\mathrm{A+B,s}} = C_{\mathrm{A+B,g}} + E_{\mathrm{A}} + E_{\mathrm{B}} - E_{\mathrm{AB}}, \qquad (6)$$

where E_{A}, E_{B}, and E_{AB} are the adsorption energies of COH_j, H, and COH_{j+1}, respectively; the term $C_{\mathrm{A+B,g}}$ represents the combination (binding) energy in the gas phase.

In addition to the reaction energies, the activation barriers should also be important factors in determining the reaction process. However, it is rather difficult to locate transition states for the surface reactions. Shustorovich [26] has developed a quite useful approach, the so-called bond-order conservation Morse-potential (BOC-MP) method to predict activation energies for dissociations or combinations of adsorbates on metal surfaces. For combination reaction (4), the formula is given by

$$\begin{aligned} E^*_{\mathrm{A+B,s}} &= \frac{1}{2}\left(\frac{E_{\mathrm{A}}E_{\mathrm{B}}}{E_{\mathrm{A}}+E_{\mathrm{B}}} + C_{\mathrm{A+B,g}} + E_{\mathrm{A}} + E_{\mathrm{B}} - E_{\mathrm{AB}}\right) \\ &= \frac{1}{2}\left(\frac{E_{\mathrm{A}}E_{\mathrm{B}}}{E_{\mathrm{A}}+E_{\mathrm{B}}} + C_{\mathrm{A+B,s}}\right). \qquad (7) \end{aligned}$$

Table 4

Calculated combination energies[a] $C_{\mathrm{A+B,s}}$ (eV) (scheme (5)) and activation barriers E^* (eV) (equation (7)) (s = surface).

	$C_{\mathrm{A+B,g}}$[b]	Cu_{10}		Pd_{10}		Pt_{10}	
		$C_{\mathrm{A+B,s}}$	E^*	$C_{\mathrm{A+B,s}}$	E^*	$C_{\mathrm{A+B,s}}$	E^*
$\mathrm{H_{2,s} \to H_s + H_s}$	(4.82)	0.59	0.83	−0.06	0.58	−0.52	0.41
$\mathrm{CO_s + H_s \to HCO_s}$	(−0.79)	0.24	0.13	0.63	0.77	0.99	1.02
$\mathrm{HCO_s + H_s \to HCOH_s}$	(−1.97)	−0.03	0.35	0.61	0.92	0.25	0.79
$\mathrm{HCOH_s + H_s \to H_2COH_s}$	(−3.37)	−1.04	0[c]	−0.78	0.13	−0.14	0.58
$\mathrm{H_2COH_s + H_s \to H_3COH_s}$	(−5.11)	−2.29	0[c]	−0.97	0.05	−0.43	0.44

[a] Dissociation energy ($D_{\mathrm{AB,s}}$) in the case of $\mathrm{H_{2,s} \to H_s + H_s}$.

[b] Calculated combination energies in the gas phase.

[c] Negative values are obtained and so they are set as zero.

Here the energy terms are shown in scheme (5). According to equation (7), the BOC-MP formula reveals a correlation between the activation and combination energies for surface reaction (4).

3.2.1. Dissociation of H_2

According to figure 1, the dissociation of $\mathrm{H_2}$ ($\mathrm{H_2 \to H_s + H_s}$) on the metal surface is an initial step. So we first examine the energetics of the dissociation. On Cu, the dissociation is mildly endothermic and shows relatively high activation energy (0.8 eV). On Pd, the dissociation is nearly thermoneutral, and on Pt it is mildly exothermic. It is clear that a smaller dissociation energy gives rise to lower activation energy.

3.2.2. The $COH_j + H$ combination

In the gas phase, the combination of COH_j and H is rather exothermic; the reaction exothermicity increases from $j = 0$ to $j = 3$. On the metal surface, the combination energies are much lower (less exothermic) because there are strong metal–COH_j and metal–H bonds. The $C_{\mathrm{A+B,s}}$ value decreases from $j = 0$ to $j = 3$, but the decrease is less pronounced than that in the gas phase. Because the adsorption bonds of the reaction species are weaker on Cu than on Pd and Pt, the combination energies on Cu are all higher (more exothermic) than those on Pd and Pt.

On Cu, the first CO hydrogenation step is slightly endothermic; the related activation is estimated to be 0.1 eV. The second step ($j = 1$) is thermoneutral and has an activation energy of 0.4 eV. The other two steps are rather exothermic. Because the –$C_{\mathrm{A+B,s}}$ values are even larger than the "reduced" adsorption energy $E_\mathrm{A}E_\mathrm{B}/(E_\mathrm{A} + E_\mathrm{B})$, negative activation energies are obtained by using the BOC-MP formula. On Pd, the first and second steps are mildly endothermic and have relatively high activation energies (0.8–0.9 eV). The other two steps are quite exothermic and have low activation energies (0.1 eV). On Pt, the first step is rather endothermic and has high activation energy (1 eV). The second step is slightly endothermic but has also rather high activation energy (0.8 eV). The other two steps are slightly exothermic; the activation energies vary between 0.4 and 0.6 eV.

For the whole process, the reaction with the highest activation energy should be the rate-determining step (RDS). So the RDS is different for the metals. On Cu, the dissociation of $\mathrm{H_2}$ is the RDS. On Pd and Pt, $\mathrm{HCO_s + H_s \to HCOH_s}$ and $\mathrm{CO_s + H \to HCO_s}$ are the rate-determining steps, respectively. On the other hand, the catalytic activity of the metal in methanol synthesis can be related to the highest activation energy. The highest E^* values show the order of Cu < Pd < Pt. The trend is consistent with the experimental fact that Cu is more active than Pd and Pt in methanol synthesis [2].

4. Conclusions

This paper presents theoretical studies of CO hydrogenation to methanol on Cu, Pd, and Pt metals. The adsorption energies for various intermediate species and the reaction energies for elementary steps involved are determined. The BOC-MP method is used to evaluate the activation energies. It is shown that CO hydrogenation to methanol is readily activated by these metals. On Cu, the dissociation of $\mathrm{H_2}$ to $\mathrm{H_s}$ is the rate-determining step because the reaction has the highest activation barrier; the combinations of $\mathrm{COH}_j + \mathrm{H}$ are energetically quite favorable, owing to the relatively small adsorption energies of COH_j and H on Cu. On Pd and Pt, the adsorption energies of H are relatively large and so, dissociation of $\mathrm{H_2}$ on the two metals proceeds easily; the hydrogenations of HCO to HCOH and CO to HCO have the highest activation barriers, respectively. The highest activation barriers vary in the order Cu < Pd < Pt, which can be related to the order of the catalytic abilities of the metals.

Acknowledgement

The work described above was fully supported by a grant from the Research Grants Council of the Hong Kong Special Administration Region, China (Project No. RGC/96-97/02). The authors are deeply indebted to Dr. M.S. Liao for his valuable comments.

References

[1] T.H. Fleisch and R.L. Mieviller, J. Catal. 90 (1984) 165.

[2] G.C. Chinchen, P.J. Denny, J.R. Jennings, M.S. Spencer and K.C. Waugh, Appl. Catal. 36 (1988) 1.

[3] M.L. Poutsma, L.F. Elek, P.A. Ibarbia, A.P. Risch and J.A. Rabo, J. Catal. 52 (1978) 157.

[4] A. Takeuchi and R. Katzer, J. Phys. Chem. 86 (1982) 2438.

[5] J.M. Thomas and W.J. Thomas, *Principles and Practice of Heterogeneous Catalysis* (VCH, Weinheim, 1997) ch. 8.

[6] F. Fischer and H. Tropsch, Brennst. Chem. 7 (1926) 97.

[7] R.W. Joyner, J. Catal. 50 (1977) 176.

[8] A. Jones and B.D. McNicol, J. Catal. 47 (1977) 384.

[9] M. Araki and V. Ponec, J. Catal. 44 (1976) 439.

[10] P. Biloen, J.N. Helle and W.M.H. Sachtler, J. Catal. 58 (1979) 95.

[11] Y. Kikuzono, S. Kagami, S. Naito, T. Onishi and K. Tamaru, Faraday Disc. Chem. Soc. 72 (1981) 143.

[12] A. Takeuchi and J.R. Katzer, J. Phys. Chem. 85 (1981) 937.

[13] E. Shustorovich and A.T. Bell, J. Catal. 113 (1988) 341;
A.T. Bell and E. Shustorovich, J. Catal. 121 (1990) 1.

[14] R.D. Srivastava, *Heterogeneous Catalytic Science* (CRC Press, Boca Raton, FL, 1988) ch. IV.

[15] R.G. Herman, K. Klier, G.W. Simmons, B.P. Finn, J.B. Bulko and T.P. Kobylinski, J. Catal. 56 (1979) 407;
S. Mehta, G.W. Simmons, K. Klier and R.G. Herman, J. Catal. 57 (1979) 339;
J.B. Bulko, R.G. Herman, K. Klier and G.W. Simmons, J. Phys. Chem. 83 (1979) 3118.

[16] S.P.S. Andrew, Post Congr. Symp. Int. Congr. Catal. 7th Osakar (1980).

[17] G.C. Chinchen, K.C. Waugh and D.A. Whan, Appl. Catal. 25 (1986) 101;
G.C. Chinchen, C.M. Hay, H.D. Vandervell and K.C. Waugh, J. Catal. 103 (1987) 79.

[18] B.S. Clausen, G. Steffensen, B. Fabius, J. Villadsen, R. Feidenhaus'l and H. Topsøe, J. Catal. 132 (1991) 524.

[19] J.B. Friedrich, M.S. Wainwright and D.J. Young, J. Catal. 80 (1983) 1.

[20] E.J. Baerends, D.E. Ellis and P. Ros, Chem. Phys. 2 (1973) 41;
G. te Velde and E.J. Baerends, J. Comp. Phys. 99 (1992) 84.

[21] S.H. Vosko, L. Wilk and M. Nusair, Canad. J. Phys. 58 (1980) 1200.

[22] A.D. Becke, Phys. Rev. A 38 (1988) 3098.

[23] J.P. Perdew, Phys. Rev. B 33 (1986) 8822.

[24] T. Ziegler, V. Tschinke, E.J. Baerends, J.G. Snijders and W. Ravenek, J. Phys. Chem. 93 (1989) 3050.

[25] C.T. Au, M.S. Liao and C.F. Ng, J. Phys. Chem. 102 (1998) 3959.

[26] E. Shustorovich, Adv. Catal. 37 (1990) 101.

[27] T.N. Rhodin and G. Ertl, *The Nature of the Surface Chemical Bond* (North-Holland, Amsterdam, 1979) ch. 5.

[28] G.E. Gdowski, J.A. Fair and R.J. Madix, Surf. Sci. 127 (1983) 541.

[29] P. Hollins and J. Pritchard, Surf. Sci. 127 (1983) 541.

[30] R.J. Behm, K. Christmann, G. Ertl and M.A. van Hove, J. Chem. Phys. 73 (1980) 2984.

[31] E. Schweizer, B.N.J. Persson, M. Tushaus, D. Hoge and A.M. Bradshaw, Surf. Sci. 213 (1989) 49.

[32] C. Zheng, Y. Apeloig and R. Hoffmann, J. Am. Chem. Soc. 110 (1988) 749.